SIAM J. Applied Dynamical Systems
Vol. 10, No. 2, pp. 452–468

Asymptotic Blowup Profiles for Modified Camassa–Holm Equations*

Robert I. McLachlan† and Xingyou (Philip) Zhang‡

Abstract. The infinite-time asymptotic behavior of a modified version of Camassa–Holm equations is studied. In order to describe the peakon-type solutions of the problem, a family of self-similar solutions of the second kind is constructed by an asymptotic analysis. Then the asymptotic profiles are compared to some numerical computations which indicate a curious property of the evolution of the solution through the asymptotic profiles.

Key words. modified Camassa–Holm equation, asymptotic profiles, solitons, blowup

AMS subject classifications. 74H35, 37K40, 35Q51

DOI. 10.1137/09076355X

1. Introduction.

In this paper, we study the asymptotic behavior of a modified version of the celebrated Camassa–Holm equations

$$m_t + um_x + 2u_x m = 0, \qquad \text{with} \quad m = (I - \partial_x^2)^k u,\ x \in \mathbb{R}^1, \tag{1.1}$$

where $k \geq 2$ is a positive integer. It is derived as the Euler–Poincaré differential equation on some Lie group with respect to the H^k metric [15]. This equation with $k = 0, 1$ corresponds to the KdV equation and the Camassa–Holm equation, respectively.

In order to study the shallow water waves, Camassa and Holm [7] derived in 1993 the partial differential equation (PDE)

$$(I - \partial_x^2)u_t + 2\partial_x u \cdot (I - \partial_x^2)u + u \cdot (\partial_x - \partial_x^3)u = 0, \tag{1.2}$$

which is now called the Camassa–Holm equation and is considered one of the most fascinating PDEs in mathematical physics. Many people have contributed to the well-posedness study on the whole real line $\mathbb{R}$ or on the unit circle S, including Arnold and Khesin [4], McKean [14], and the references therein. The Camassa–Holm equation admits smooth solutions and the so-called soliton (peakon) solutions as well.

Following the ideas introduced by Arnold [3], which view the Euler fluid equation as the geodesic on some diffeomorphism group, Khesin and Misiołek [11] have proven that the KdV equation and the Camassa–Holm equation are the equations of the geodesic flow associated to the L^2 and H^1 metrics, respectively, on the Bott–Virasoro group $\widehat{\mathcal{D}}^s(S)$ of the unit circle $S = [0, 2\pi]$.

*Received by the editors July 1, 2009; accepted for publication (in revised form) by T. Kaper March 10, 2011; published electronically May 26, 2011.
http://www.siam.org/journals/siads/10-2/76355.html
†Institute of Fundamental Sciences, Massey University, Palmerston North, New Zealand (R.McLachlan@massey.ac.nz).
‡Applied Maths Team, Industrial Research Ltd, Lower Hutt, New Zealand (p.zhang@irl.cri.nz; zxy.cqu@gmail.com).

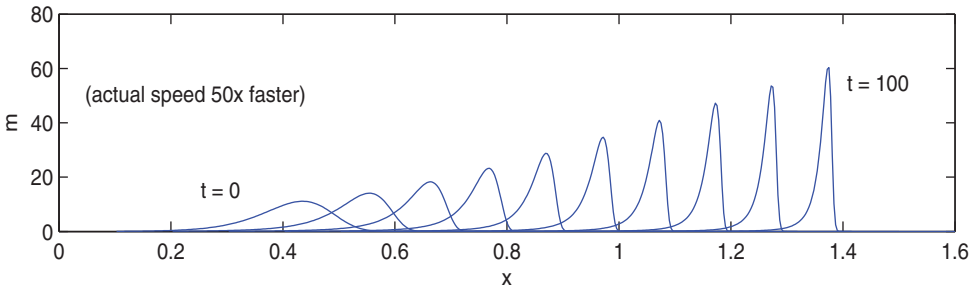

Figure 1. *The evolution of Gaussian initial value. The snapshots are taken at equal time intervals.*

Now it is natural to ask how the dynamics of the geodesic flows on the Bott–Virasoro group depends on the H^k metric from which the geodesic equations are derived. This leads us to our study [15] on (1.1), where we derived the PDE and studied its well-posedness. One of the results there is the following proposition.

Proposition 1.1. *Suppose $k \geq 2$ in (1.1). If the initial value $m(0,x) \in L^2(S)$, then $m(t,x) \in L^2(S)$ for any finite time $t > 0$, and there exists a constant C_0 depending only on the norm of initial values u such that*

$$||m||_{L^2} \leq e^{C_0 t}||m_0||_{L^2}. \tag{1.3}$$

Similar results also hold true for the whole line $\mathbb{R}$ case [15]. This means that there is no finite-time blowup for (1.1) if the initial value is smooth enough. This is quite different from the nature of the Camassa–Holm equation, because we know that for the Camassa–Holm equation, even some very smooth initial values may lead to the finite-time blowup solution, i.e., the momentum m may blow up to a δ function in finite time.

On the other hand, one of the most interesting things for the generalized Euler equations on Lie groups is that they admit the particle solutions, examples of which include the point vortices in the Euler fluid equations and the peakons in the Camassa–Holm equation. In a recent survey [10] on this, Holm and Marsden studied the dynamics of the so-called singular momentum map solutions. The numerical simulations indicate that this kind of solution even dominates the time asymptotic dynamics of the initial value problems [10]. The authors of [7, 8] studied the integrable solitons on the real line and Alber et al. studied in [1, 2] the integrable solitons on the periodic case. In [9], Fringer and Holm studied the behavior of some integrable and nonintegrable geodesic solitons, i.e., the equation

$$m_t + um_x + 2mu_x = 0, \qquad m = Qu,$$

with different inertia operators Q. They observed the emergence of the singular momentum map solutions (which they called "pulsons") in their numerical study, and they also studied the interactions of these pulsons.

Our numerical simulation for solving (1.1) in [18] strongly suggests that (1.1) has some solutions that blow up at $t = \infty$, although it has no finite-time blowup solution. See Figure 1 for the evolution of the solution m with the Gaussian initial value m_0. This indicates that, for the modified Camassa–Holm equation (1.1), the singular momentum map solutions also dominate the evolution of the confined solutions.

We use the term *weak blowup* to describe this kind of blowup at $t = \infty$, and this paper is mainly concerned with the asymptotic profile analysis of the weak blowup. We obtain the asymptotic profiles for the weak blowup, and then we try to understand numerically how the confined initial value blows up to the δ momentum. Our numerical results agree with the asymptotic theory, and at the same time they show evidence for quite a curious property on the asymptotic profiles through which the solution m evolves toward the Dirac δ momentum.

2. Asymptotic PDEs. In general, if we know that an evolutionary PDE has a solution $v(x,t)$ which blows up at time T and we are to study the (asymptotic) self-similar blowup profile f for the solution $v(x,t)$ of the PDE, we need to choose an appropriate "similarity variable ξ," which may depend on x and t, and a scaled factor $\phi(t)$ (may depend on T) according to the nature of PDE such that when plugging the solution $v(x,t) = \phi(t)f(\xi)$ into the PDE, we can obtain a differential equation of f as t goes to the blowup time T. The traveling wave solutions of PDEs are closely related to the self-similar solutions which Barenblatt [5] discussed intensively for PDEs. Here by the term "traveling wave" we mean the solutions of the form $f(x-ct)$. If one is looking for traveling wave solutions $u(t,x) = f(x-ct)$, then one can regard $\xi = x - ct$ as a new variable and plug this ansatz $u(t,x) = f(x-ct)$ back into the PDE to get an ODE in ξ.

For some PDEs, the resulting differential equation on f has a unique (stable) solution (see e.g., [12, 13] for the generalized KdV equations and [17] for traveling wave solutions of parabolic systems); then one can use various tools to prove that the solution of the PDEs goes to the unique steady solution in some sense.

But for (1.1), we will find in this paper that the situation is quite different.

In order to study how the solutions are approaching the blowup profile, we consider the traveling wave solutions of the form

$$m(t,x) = \phi(t)f(\phi(t)\cdot(x-ct))$$

with a scaling factor $\phi(t)$ (we take this form to guarantee $\int_{\mathbb{R}} m = \int_{\mathbb{R}} f$). We will first plug this ansatz into (1.1) to find the right choice of $\phi(t)$ and then get the differential equation that f satisfies.

If G denotes the Green's function for the operator $(1-\partial_x^2)^k$, then, for very large $\phi = \phi(t)$, we can approximate u by (if we denote $\xi = \phi\cdot(x-ct)$, $\eta = \phi\cdot(y-ct)$)

$$\begin{aligned} u(y) &= \int_{\mathbb{R}} G(y-x)m(x)\mathrm{d}x = \int_{\mathbb{R}} G\left(\frac{\eta-\xi}{\phi}\right) f(\xi)\mathrm{d}\xi \\ &= \int_{\mathbb{R}} \left(G_0 + \frac{(\eta-\xi)^2}{2\phi^2}G''(0)\right) f(\xi)\mathrm{d}\xi + O\left(\frac{1}{\phi^3}\right) \quad \text{with } G_0 = G(0) \\ &= G_0 f_0 + \frac{G''(0)}{2\phi^2}f_2 + \frac{G''(0)}{2\phi^2}f_0\eta^2 - \frac{\eta}{\phi^2}G''(0)f_1 + O\left(\frac{1}{\phi^3}\right), \end{aligned} \tag{2.1}$$

where $f_i = \int_{\mathbb{R}} \xi^i f(\xi)\mathrm{d}\xi$. Here we have used the fact that $G'(0) = 0$. From (2.1), we have for

very large ϕ that

$$\begin{aligned} u_y &= \int_{\mathbb{R}} G'_y(y-x)m(x)\mathrm{d}x \\ &= G''(0)(\eta f_0 - f_1)/\phi + O\left(\frac{1}{\phi^2}\right). \end{aligned} \tag{2.2}$$

Substituting (2.1)–(2.2) into (1.1), we get a differential equation

$$\begin{aligned} &\phi f' \cdot (\phi'\eta/\phi - c\phi) + \phi' f + 2G''(0)(\eta f_0 - f_1)f \\ &\qquad + \left(G_0 f_0 + \frac{G''(0)}{2\phi^2} f_2 + \frac{G''(0)}{2\phi^2}\eta^2 f_0 - \frac{G''(0)}{\phi^2}\eta f_1\right)\phi^2 f' = 0, \end{aligned} \tag{2.3}$$

i.e.,

$$\eta f'\phi' - cf'\phi^2 + f\phi' + G_0 f_0 f'\phi^2 + 2G''(0)(\eta f_0 - f_1)f + \frac{G''(0)}{2}\left(f_2 + \eta^2 f_0 - 2\eta f_1\right) f' = 0. \tag{2.4}$$

In order to make this equation balance in ϕ, we have to assume $\phi' \sim 1$ or $\phi' \sim \phi^2$. We will discuss which assumption suits our need.

- If $\phi' \sim \phi^2$, take $\phi' = \phi^2$ as an example; then $\phi(t)$ will become infinity at some finite time, which contradicts with Proposition 1.1. Moreover, if $\phi' = \phi^2$, then the leading term in (2.4) will lead to

  $$\eta f' - cf' + f + G_0 f_0 f' = 0,$$

  which has only unbounded solutions. This is not of interest to us because we are looking for some smooth profile. This rules out the choice $\phi' \sim \phi^2$.
- If $\phi' \sim 1$ (take $\phi(t) = t$, for example) we can get the case in which we are interested. See Remark 1 for an explanation on what we can obtain from the general choice $\phi(t) = A(t + B)$ of the solution of $\phi' \sim 1$.

Now assume $\phi(t) = t$; then we match the coefficients of t^i in (2.4):

$$\begin{aligned} t^0: &\quad \left[2G''(0)(\eta f_0 - f_1) + 1\right] f \\ &\qquad + \left(\frac{G''(0)}{2} f_2 + \frac{G''(0)}{2}\eta^2 f_0 - G''(0)\eta f_1 + \eta\right) f' = 0, \\ t^2 = \phi^2: &\quad -cf' + G_0 f_0 f' = 0. \end{aligned}$$

The leading order term $t^2(-cf' + G_0 f_0 f')$ is the limiting (δ function) part of the motion. If we divide (2.3) by t^2 and let $t \to \infty$, then we get $-cf' + G_0 f_0 f' = 0$, which means the leading order term determines the speed c of the soliton: $c = G_0 f_0$. If we denote $U(\eta) = \frac{1}{2}G''(0)f_0\eta^2 - G''(0)f_1\eta + \frac{1}{2}G''(0)f_2$, then the ODE for the coefficient in t^0 takes the form

$$(\eta f)_\eta + f_\eta U + 2U_\eta f = 0. \tag{2.5}$$

This equation is nonlinear and nonlocal (for U depends on the integrals of f), but fortunately it can be explicitly solved as follows.

Multiplying the left-hand side of the ODE in t^0 by η and then integrating it, we find that $f_1 = 0$. Now that $f_0 = \int_{\mathbb{R}} f = \int_{\mathbb{R}} m$ is a conserved quantity for (1.1), and $G''(0) < 0$, so without loss of generality we can assume $f_0 G''(0) = -1$. Then f_2 turns up as a parameter. In order to simplify the notation, we introduce a parameter a out from f_2 by $f_2 G''(0) = -1 - a^{-2}$; then we have

$$(-2\eta + 1)f + \frac{1}{2}(2\eta - \eta^2 - 1 - a^{-2}) \cdot f' = 0, \tag{2.6}$$

and so

$$\frac{\mathrm{d}f}{f} = \frac{-2(2\eta - 1)\mathrm{d}\eta}{(\eta - 1)^2 + a^{-2}};$$

then

$$-\frac{\mathrm{d}f}{f} = \frac{2 + 4(\eta - 1)}{(\eta - 1)^2 + a^{-2}}\mathrm{d}\eta = \frac{2}{(\eta - 1)^2 + a^{-2}}\mathrm{d}\eta + \frac{4(\eta - 1)}{(\eta - 1)^2 + a^{-2}}\mathrm{d}\eta.$$

From this we have

$$f(a, \eta) = C(a) \cdot \frac{e^{-2a[\arctan(a(\eta - 1)) + \frac{\pi}{2}]}}{((\eta - 1)^2 + a^{-2})^2}. \tag{2.7}$$

We can find, with the help of the software Mathematica, that

$$\int_{-\infty}^{+\infty} f\mathrm{d}\eta = \frac{C(a)a^2}{4}\frac{1 - e^{-2a\pi}}{a^2 + 1}, \qquad \int_{-\infty}^{+\infty} \eta^2 f\mathrm{d}\eta = \frac{C(a)}{4}(1 - e^{-2a\pi}).$$

If we take

$$C(a) = -\frac{1}{G''(0)}\frac{a^2 + 1}{a^2} \cdot \frac{4}{1 - e^{-2a\pi}},$$

then f does satisfy the conditions $f_0 G''(0) = -1$, $f_2 G''(0) = -1 - a^{-2}$. The limit of (2.7) is

$$\lim_{a \to +\infty} f(a, \eta) = \tilde{f} = \begin{cases} \dfrac{-4}{G''(0)}(\eta - 1)^{-4} e^{\frac{2}{\eta - 1}} & \text{if } \eta - 1 < 0, \\ 0 & \text{if } \eta - 1 > 0. \end{cases} \tag{2.8}$$

Here in (2.7), we have taken an integral constant $C(a)e^{-a\pi}$ in order to guarantee the limit function $\tilde{f} \in L^1(\mathbb{R})$. It is easy to verify that $\tilde{f}$ is a solution to (2.5), too, and we call this solution the *limit steady solution*. The steady solutions with G being the Green's function of $(I - \partial_x^2)^2$ are depicted in Figure 2.

Some remarks are in order at this stage.

Remark 1. The general solution to $\phi'(t) \sim 1$ is

$$\phi(t) = A(t + B)$$

for arbitrary constants A and B. If we take $A = 1$, then we still have the same asymptotic equation as (2.5) even if we take $B \neq 0$. So the introduction of an arbitrary constant B does not change the asymptotic stationary equation. Now if we take $\phi(t) = At$, then the asymptotic stationary equation reads

$$A(\eta f)_\eta + f_\eta U + 2U_\eta f = 0 \tag{2.9}$$

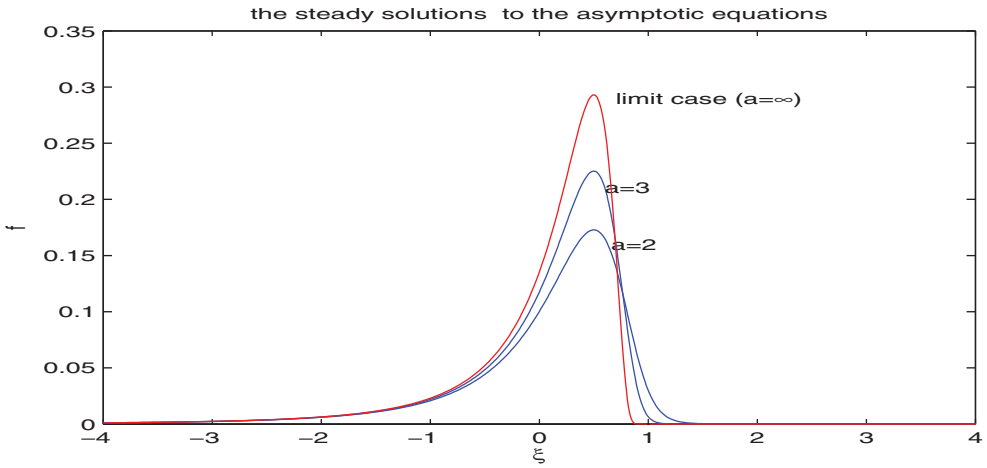

Figure 2. *The steady solutions to the asymptotic equations.*

with $U(\eta) = \frac{1}{2}G''(0)f_0\eta^2 + \frac{1}{2}G''(0)f_2$. However, due to the special form of (2.9), we can see that with the stretching transform $\eta \mapsto \alpha\eta$, $f \mapsto \alpha f$ (and correspondingly $f_2 \mapsto \alpha^2 f_2$, $U \mapsto \alpha^2 U$, $U_\eta \mapsto \alpha U_\eta$) with $\alpha = A$, equation (2.9) is transformed into (2.5). This means that the real asymptotic profiles are a two-parameter family: one parameter a is for the shape of the profile, and the other one α (or A) is for the spatial stretching factor.

Remark 2. There are two very interesting features of (2.5).

- Equation (2.5) is a nonlinear differential equation, so in general we cannot multiply or divide the solution by a constant to get a solution. But once we know f_0 is fixed from the conservation law of (1.1), then f_2 (or a) turns out to be a parameter defining the shape of the solution, and (2.5) can be solved explicitly.
- The other interesting point here is that there is a family of one-parameter self-similar blowup profiles (or a family of two-parameter profiles for (2.9)), unlike in most familiar cases where only a unique profile exists [12, 13, 17]. This is what Barenblatt called a self-similarity solution of the second kind in [5], which means that one cannot obtain this kind of solution only by dimensional analysis.

Now that we have the asymptotic stationary profiles, can we say something about the asymptotic evolution of the solution to (1.1) toward the profiles in an *intrinsic slow-time* scale? That is, if we take $m(x,t) = tf(t(x-ct),\tau)$, with a time scale factor $\tau = g(t)$ (here we again omit the stretching factor A in $m(x,t) = Atf(At(x-ct),\tau)$), then we can do the same things as before:

$$stf_\xi \cdot (\eta/t - ct) + f + tf_\tau g'(t) + 2G''(0)(\eta f_0 - f_1)f + \left(G_0 f_0 + \frac{G''(0)}{2t^2}f_2 + \frac{G''(0)}{2t^2}\eta^2 f_0 - \frac{G''(0)}{t^2}\eta f_1\right) t^2 f_\xi = 0. \tag{2.10}$$

This means that if we want to take f_τ into the equation, we have to take $g'(t) = \frac{1}{t}$, that is, $g(t) = \ln t$. Then we have the following asymptotic slow-time PDE (the self-similar case):

$$f_\tau + (\xi f)_\xi + Uf_\xi + 2U_\xi f = 0, \tag{2.11}$$

where $U = \frac{G''(0)}{2}(\xi^2 f_0 - 2\xi f_1 + f_2)$. It is easy to verify that f_0 is independent of t, from which we can assume $f_0 G''(0) = -1$ in order to simplify the calculation.

The numerical simulation strongly suggests that the steady solutions (2.7) and (2.8) are stable for the asymptotic equations (2.11) and are stable asymptotic solutions to (1.1) (here we use the term "stable asymptotic solutions" to mean that the solutions of (1.1) tend to the family of "steady solutions" (2.7) and (2.8), but we have to point out that (2.7) and (2.8) are not the steady solutions of (1.1), although they are the steady solutions of (2.11)).

3. Boundary conditions for the inner problem via matched asymptotic expansions. If we linearize (2.11) around the steady solution f by a small perturbation $f + \varepsilon h(\tau, \xi)$, we get the linearized equation on h

$$h_\tau + [(U + \xi)h]_\xi + U_\xi h + (Wf)_\xi + W_\xi f = 0, \tag{3.1}$$

where $U = \frac{G''(0)}{2}(f_0\xi^2 + f_2)$, $W = \frac{G''(0)}{2}(h_0\xi^2 - 2h_1\xi + h_2)$, and $h_i = \int \xi^i h(\xi)\mathrm{d}\xi$. Multiplying (3.1) by ξ^i, $i = 0, 1, 2$, and integrating by parts, one can easily find that

$$\frac{\mathrm{d}h_0}{\mathrm{d}\tau} = 0, \quad \frac{\mathrm{d}h_1}{\mathrm{d}\tau} = h_1, \quad \frac{\mathrm{d}h_2}{\mathrm{d}\tau} + \frac{G''(0)}{2}(h_0 f + f_0 h)\xi^4 \Big|_{-\infty}^{+\infty} = 2h_2. \tag{3.2}$$

We can see that some characteristics of (3.1) cannot reach the ξ axis (i.e., $\tau = 0$) (see Figures 3 and 4), so if we want to solve (2.11) (or 1.1) reliably, we need some appropriate upstream boundary conditions $f(\tau, \xi_0)$ for some large ξ_0; for example, we need as the upstream boundary condition

$$\lim_{\tau \to \infty} f(\tau, \xi_0) = 0 \quad \text{for very large } \xi_0 \tag{3.3}$$

in order that the small perturbations from the upstream do not affect the solution in the *inner region*, i.e., where $\xi \sim O(1)$, by the propagation along the characteristics.

Up until now, we have taken $\xi = t(x - ct)$, with $c = G(0)f_0$, as a new variable, which means that we concentrate on the region where the bump is supported and which is getting thinner as t increases. Now we are going to obtain some upstream boundary conditions for

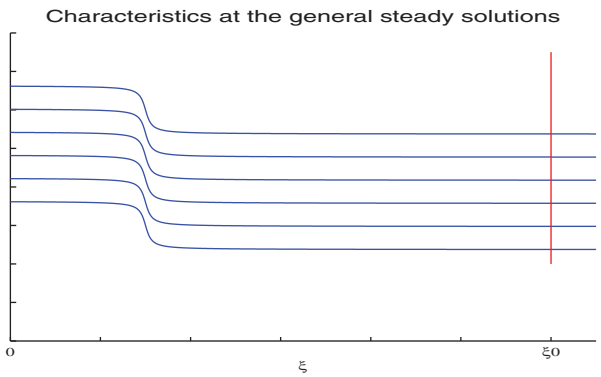

Figure 3. *Characteristics of the linearized equations around the general steady solutions.*

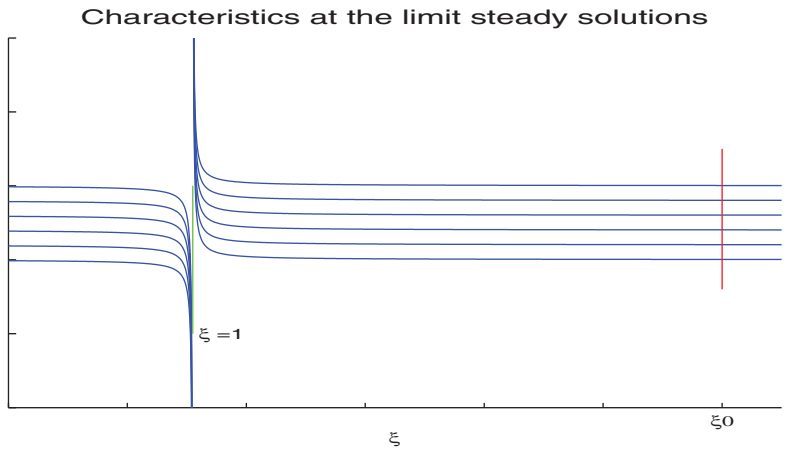

Figure 4. *Characteristics of the linearized equations around the limit steady solution.*

(2.11) and (3.1), that is, the boundary condition for very large ξ, where the so-called matched asymptotic expansion method comes in.

The technique of matched asymptotic expansion concerns different differential equations in two regions known as the "fine scale" (or inner) region and the "coarse scale" (or outer) region, matching the boundary condition on the "common" boundary (see [5] and [16], etc., for details). The multiscale asymptotic expansion is very subtle. One has to be very careful to choose the inner/outer variables in order to have the useful relations. If one chooses a wrong scale, then the resulting equations may not make sense or may contradict each other. The key point is the scale under which the problem is considered or, in other words, what limit process is of interest to us. Specific to our problem here, we can think of the region A with the variable $\xi = t(x - ct)$ as the inner region (with $\xi = O(1)$) and think of the region out of A as an outer region with another, much coarser, variable, for example, $z = x - ct = O(1)$. Now that we need the up-stream boundary condition for $f(\xi, \tau)$ or $h(\xi, \tau)$, we can think of this as the boundary condition at $z \to 0^+$ of the outer region equation as $t \to +\infty$ (see Figure 5).

So we introduce $z = x - ct$ as a new variable and have another approximation for $u(x)$ in (1.1) (when t is very large, while we think $z = x - ct = O(1)$, because now we are in the z coordinate):

$$\begin{aligned} u(y) &= \int_{\mathbb{R}} G(y-x)m(x)\mathrm{d}x \\ &= \int_{\mathbb{R}} G\left(y - ct - \frac{\xi}{t}\right) f(\xi)\mathrm{d}\xi \quad \text{if } m(x) = tf(t(x-ct)),\ \xi = t(x-ct),\ c = G_0 f_0 \\ &\approx G(y-ct)f_0 - \frac{1}{t}\cdots, \end{aligned} \tag{3.4}$$

and so in a moving frame (which means we can let $z = x - ct$ denote the relative position of the point x with respect to the point where the Dirac δ function is supported, and consider m as a function of z : $m(t,x) = n(t,z) = n(t,x-ct))$, $m(0,x) = n(0,z) = n(0,x)$ and $m_t = n_t - cn_z$. If we denote $v(z) = (G(z) - G_0)f_0$, then $v(z) = u(x) - c$, $v_z = u_x$, and we can

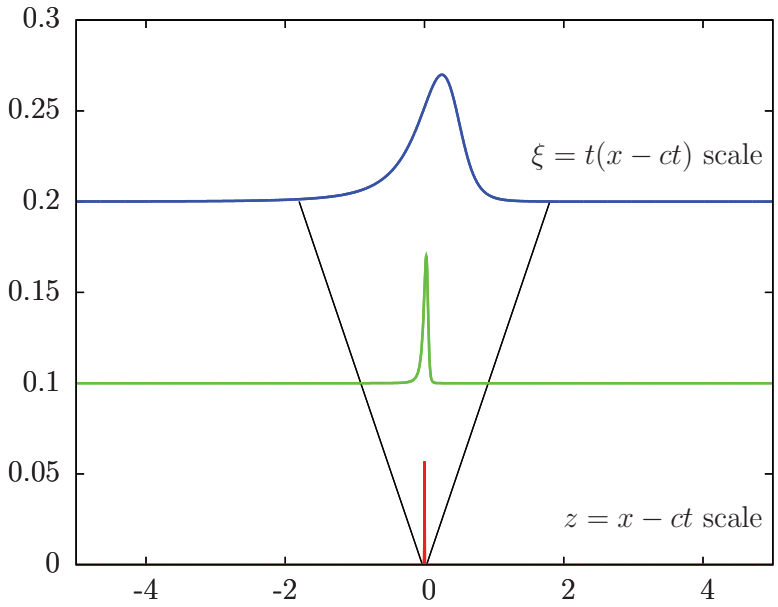

Figure 5. *A schematic illustration of the inner and outer regions. As $t \to \infty$, any bounded interval of the ξ-region corresponds to a point in the z-region.*

approximate (1.1) (in the region where t is large enough and $z = x - ct = O(1)$) by

$$n_t + vn_z + 2v_z n = 0. \tag{3.5}$$

If we take $f_0 = 1$ just for simplifying the notation, then $v(z) = (G(z) - G_0)f_0 = G(z) - G_0$. It is easy to find that the characteristics curve $z = F(t, z_0)$ for (3.5) is defined by

$$\int_a^z \frac{1}{G(x') - G_0} \mathrm{d}x' = t + \int_a^{z_0} \frac{1}{G(x') - G_0} \mathrm{d}x', \tag{3.6}$$

where

$$a = \begin{cases} 1 & \text{if} \quad z_0 > 0, \\ -1 & \text{if} \quad z_0 < 0. \end{cases}$$

$z = F(t, z_0)$ means that the curve starting from z_0 at $t = 0$ gets to z at time t, so it is clear that $z_0 = F(-t, z)$.

From this, one can solve (3.5) explicitly:

$$\begin{aligned} n(t, z) &= n(0, F(-t, z)) \left(\frac{G_0 - G(F(-t, z))}{G_0 - G(z)} \right)^2 \\ &= m(0, F(-t, z)) \left(\frac{G_0 - G(F(-t, z))}{G_0 - G(z)} \right)^2 \\ &= m_0(F(-t, z)) \left(\frac{G_0 - G(F(-t, z))}{G_0 - G(z)} \right)^2, \end{aligned} \tag{3.7}$$

where $z = F(t, z_0)$ is the characteristics curve.

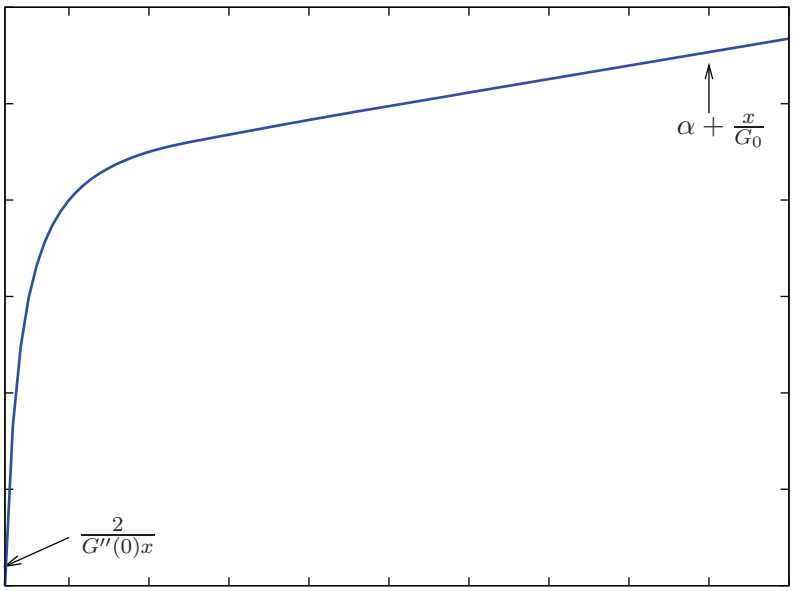

Figure 6. *Asymptotic for the function* $f(x) \equiv -\int_1^x \frac{1}{G(x')-G_0}\mathrm{d}x'$.

Now we are going to use the limit of $m(t,z)$ as $t \to +\infty$ and $z \to 0^+$ as the boundary condition of the outer region with (z,t) coordinates and then transfer this limit to the upstream boundary condition of the inner region with (ξ,τ) coordinates.

In order to do that, we need to find the asymptotic expression of $m(t,z)$ as $z > 0$ very small and t is large enough; i.e., we are interested in the case $z \to 0^+$ and $t \to \infty$ such that $\xi = zt = t(x-ct) > 0$ very large. We are concerned with how fast the initial value $m_0(z_0)$ decreases as $z_0 \to +\infty$ can guarantee that the upstream boundary conditions of $f(\xi,\tau)$ tend to 0 as $\tau \to +\infty$, and so we consider the situation where $z_0 \to +\infty$, $z \to 0^+$, $t \to +\infty$. In this case, taking into account that $G(z) = G_0 + \frac{1}{2}G''(0)z^2 + o(z^3)$ for $z > 0$ small enough and $G(z) \to 0$ as $z \to +\infty$, we have

$$-\int_1^z \frac{1}{G(x')-G_0}\mathrm{d}x' \approx \frac{2}{G''(0)z} \quad \text{is negatively large as } z > 0 \text{ small enough,} \tag{3.8}$$

$$-\int_1^{z_0} \frac{1}{G(x')-G_0}\mathrm{d}x' \approx \left(\alpha + \frac{z_0}{G_0}\right) \quad \text{is positively large as } z_0 \text{ large enough} \tag{3.9}$$

(see Figure 6). On the other hand, from (3.6) and (3.8), we have

$$-\int_1^{z_0} \frac{1}{G(x')-G_0}\mathrm{d}x' \approx \frac{1}{z}\left(tz + \frac{2}{G''(0)}\right),$$

which, together with (3.9), gives us that $z_0 \approx \frac{G_0}{z}(tz + \frac{2}{G''(0)})$, and

$$
\begin{aligned}
m(t,x) = n(t,z) &= m_0(z_0)\left(\frac{G_0 - G(F(-t,z))}{G_0 - G(z)}\right)^2 \\
&\approx \frac{G_0^2}{(G_0 - G(z))^2} m_0\left(\frac{G_0}{z}\left(tz + \frac{2}{G''(0)}\right)\right).
\end{aligned} \tag{3.10}
$$

This approximation holds true for t large enough and $z > 0$ small enough. Now we will match this $m(t,z)$ to the upstream boundary condition of $f(\xi,\tau)$. Notice $G(z) - G(0) = \frac{G''(0)}{2}z^2 + o(z^3)$ as $z \to 0^+$, so the estimate (3.10), together with $m = tf(\xi,\tau), \tau = \ln t, \xi = zt$, yields that for large ξ and τ,

$$
f(\tau,\xi) \sim e^{3\tau}\xi^{-4}\left(\frac{2G_0}{G''(0)}\right)^2 m_0\left(G_0 e^{\tau} + 2\frac{G_0 e^{\tau}}{G''(0)\xi}\right). \tag{3.11}
$$

This gives an $f(\tau,\xi)$ such that $\lim_{\tau\to\infty} f(\tau,\xi) = 0$ as long as the initial $m_0(x) = o(x^{-3})$ as $x \to +\infty$. We call this $f(\tau,\xi)$ for large $\xi = \xi_0$ the *upstream boundary condition* for the *inner problem* (2.11). From the above derivation, we can see that (3.3) is satisfied as long as the initial value $m_0(x)$ decays fast enough as $x \to +\infty$.

4. The family of steady solutions. Now we turn to the numerical simulation. Take $k = 2$ in (1.1) as an example (the numerical simulation for (2.11) presents similar results). We found that the real profile for the confined initial value seems to be approaching the asymptotic profiles very quickly, as shown in Figures 7–9. In these figures, the differential equation (1.1) is solved by the box scheme with a moving frame; i.e., we use $u - \max_x(u)$ as our velocity function u in the simulation and concentrate on the region where the blob is mainly supported. This region is $[0, L] = [0, 4]$, with $n = 480$ grid points, $\mathrm{dt} = 0.002$, and the initial value $m_0(x) = 8e^{-64|x-2|^2}$, which implies that (3.3) holds true. The solid line of the top plot of each figure stands for the real solution $m(x,t)$, and then we use the nonlinear least square method to solve a parameter optimization problem to find the closest profile (hence the shape parameter a) from the family

$$
a_3 e^{a_4}\frac{\exp(-2a_2\arctan(a_2a_3(x-a_1)))}{((a_3(x-a_1))^2 + a_2^{-2})^2}, \tag{4.1}
$$

with four parameters $a_i,\ i = 1,\ldots,4$: a_1 is a constant whose introduction is due to the space translation symmetry of (1.1); a_2 is the shape parameter a in the previous sections; a_3 is the spatial scaling factor, i.e., the constant A in Remark 1 of section 2 (in other words, we think $Cf(Cx)$ and $f(x)$ stand for the same profile in the family); and a_4 is the height scaling factor, and the introduction of a_4 means that we care about only the profile of the solution and not the height of the solution, which is due to the time translation symmetry of (1.1) (in other words, we identify $Cf(x)$ with $f(x)$ in the profiles). The dotted line in the figures corresponds to the best-fit profiles. We can see from Figure 1 and Figures 7–9 that the Gaussian initial value evolves very quickly to the family of steady solution profiles. Then it does not stay at any steady solution; instead, it wanders in this family of steady solutions (see the evolution of

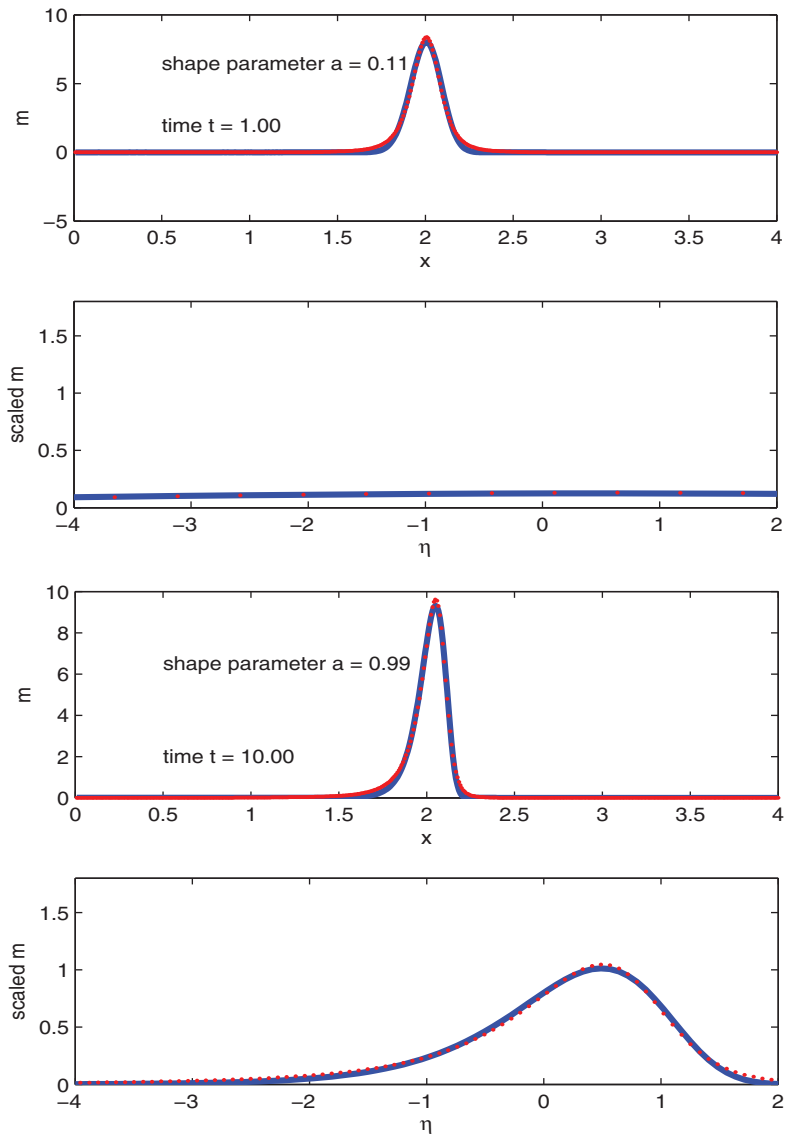

Figure 7. *Fit of the solution to the family of profiles: The equation is solved by the box scheme with a moving frame. Starting off from the Gaussian initial value, the solution is soon almost indistinguishable from the best-fit profile. Grid number* $n = 480$.

a in Figure 10). If we go a little bit further on how the shape parameter a evolves, we observe an interesting phenomena: a steadily increases for a while, and then it stops increasing at the moment when the scaled m starts to wiggle (see Figure 9 and the blue curve in Figure 10 for $n = 480$), which means that at this stage the resolution of m is not fine enough to find a good best-fit approximation from the asymptotic family. If we change the resolution of the space grid, we can find that this change does affect a (see Figure 10), and it seems to indicate that the limit asymptotic profile (2.8) is most likely the stable profile for (1.1), although we have not found rigorous proof for that.

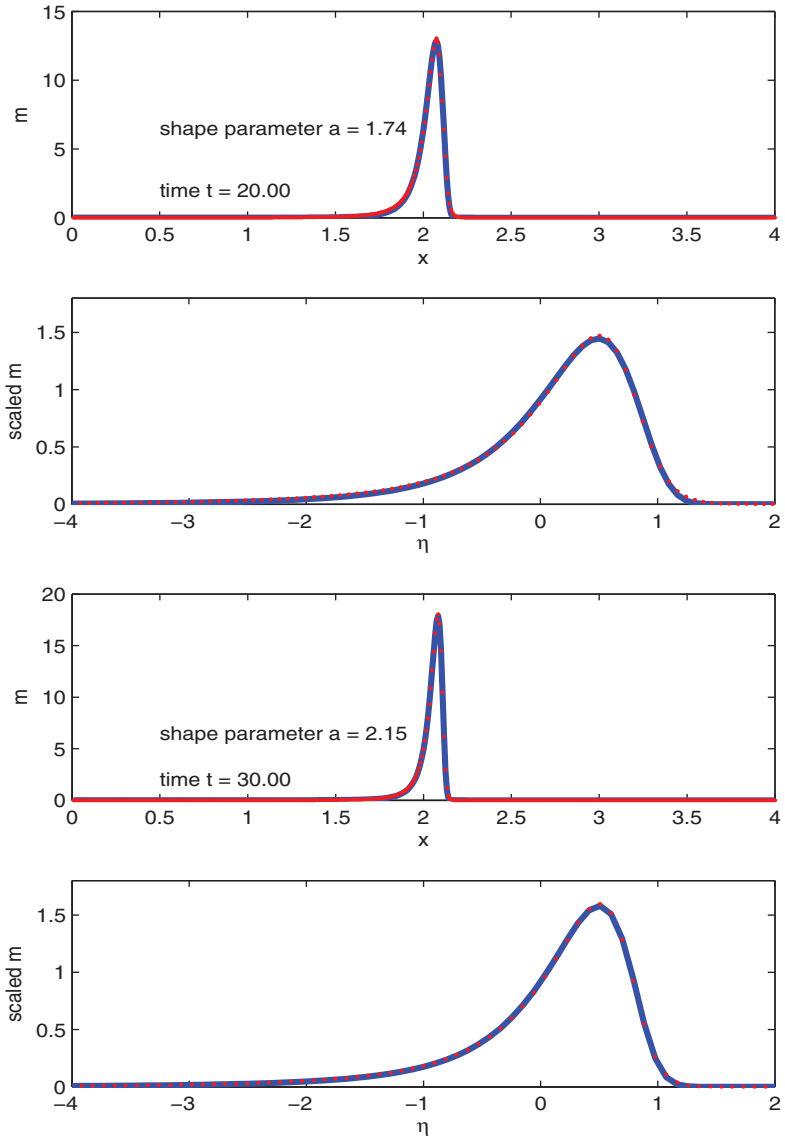

Figure 8. *Fit of the solution to the profiles. Grid number* $n = 480$.

Figure 11 is about the prediction of the constant velocity of the traveling wave; the real velocity u is quite close to $G(0)\int f$ (which is $f_0/4$ for $(I - \partial_x^2)^2$) after a short time period. We can see that some of the initial mass is left behind or smeared out of the interval where our numerical simulation continues to dwell. If we change the value A in the initial value $m(x,0) = A\exp(-A^2|x|^2)$, we observe that as A gets bigger and bigger, the velocity gets closer and closer to $G(0)m_0$.

Our numerical simulations agree with our asymptotic analysis in section 2. But we have to admit here that we have not yet rigorously solved this problem. For example, we have not found a rigorous proof that the (limiting case) δ momentum solution is (asymptotically)

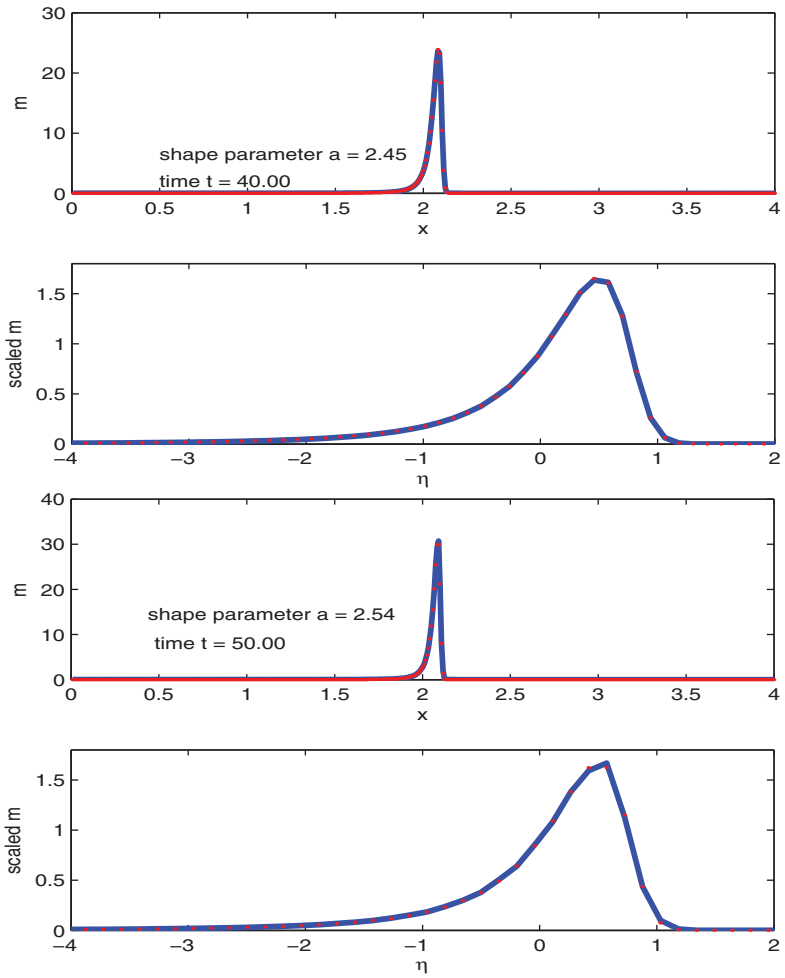

Figure 9. *Fit of the solution to the best-fit profiles: The solution is getting concentrated on a narrower region as t increases. From $t = 40.0$, the grid is not fine enough in the support region in order to obtain a decent solution and the graph starts to wiggle, as can be seen from the plot of the scaled m. Grid number $n = 480$.*

stable for either (1.1) or (2.11), although the numerical evidence indicates so. Here are some reasons why we have not found a rigorous proof:

- Analytically, both the original PDE (1.1) and its slow time asymptotic PDE (2.11) are nonlinear and nonlocal, and they are not really hyperbolic equations. In general, when talking about the stability of a steady solution, we need some nice properties such as the dissipation or some sufficient number of conserved quantities to prove that the solutions of the PDE evolve to the steady solution in some sense, but the PDEs (1.1) and (2.11) do not have such nice properties. We have studied the four-particle systems corresponding to (1.1) in [18] and obtained that only one Lyapunov exponent is positive, which indicates that there may be another conserved quantity in addition to $\int u$ and $\int um$, and it might help to prove the stability of the steady solution if we had the third conserved quantity.

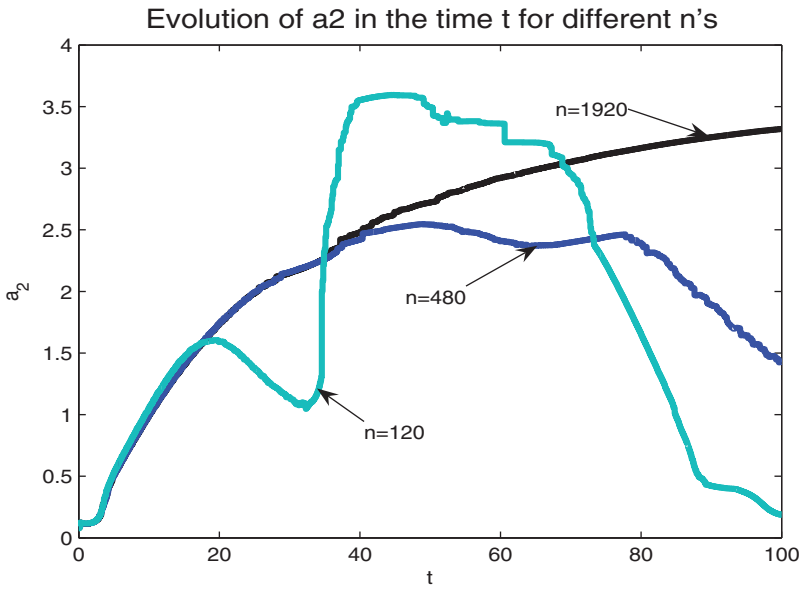

Figure 10. *The evolution of a in t for different grid resolutions $n, [0, L] = [0, 4]$; n is the number of the subintervals of $[0, L]$. The resolution $n = 120$ gives a decent solution up to $t = 16$, and $n = 480$ corresponds to the time up to $t_1 = 40$, and $n = 1920$ yields a larger time. After these times t_0, t_1, etc., the grids are not fine enough, and if we still want to find some best-fit profile for the computed solutions, then the best-fit profiles (also the shape parameter a_2) are no longer reliable.*

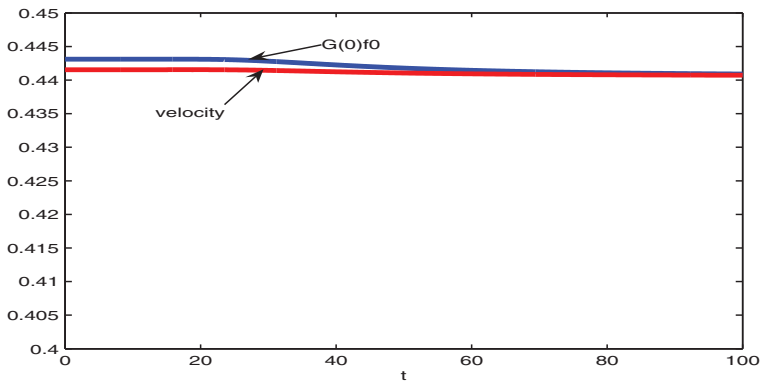

Figure 11. *The velocity of traveling wave and $G(0)m_0$. The simulation is for (1.1) with initial value $m(x, 0) = 8\exp(-64|x - 2|^2)$; the simulation interval $= [0, 4]$.*

- Numerically, the features of (1.1) and (2.11) prevent us from reliably resolving the stability of steady solutions: (a) The coefficients of (2.11) depend on f_i, $i = 0, 1, 2$. We know the solution $f(\eta, \tau)$ of (2.11) behaves like (2.7) or (2.8) after some time, which means for some $\tau_0 > 0$,

$$f \sim \eta^{-4} \qquad \text{for } |\eta| \text{ large}, \tau > \tau_0.$$

This incurs an $O(\frac{1}{L})$ error when we replace $f_2 = \int_{-\infty}^{\infty} \xi^2 f(\xi) \mathrm{d}\xi$ with the evaluation of

$f_2 = \int_{-L}^{L} \xi^2 f(\xi) \mathrm{d}\xi$ in the simulation. This error in the coefficients will take over the true solution. (b) The nature of the weak blowup of (1.1) laid a barrier to numerically solving (1.1) for a long time. As time increases, the solution, mainly supported in a narrower and narrower region, becomes larger and larger. So, if we use a fixed-grid-number approach, no matter how big the grid number we choose, the resolution of the grid is not fine enough to get a decent solution after some time. See Figure 9, where we choose $n = 480$ grid points; the grid is not fine enough after $t = 40.0$. (c) If we use a moving frame in the simulation, then we concentrate on the very narrow region where the bump is supported, which is good. But a moving frame means that we are not capturing the correct upstream boundary conditions. It seems that it would need the adaptive grid method used by Budd and Williams [6] which we could not get to work.

From the numerical simulations, we make the following conjectures:

- The two-parameter family of the steady solutions is exponentially stable; every initial value not in but close to this set will tend to it very quickly and then wander along this set.
- If the initial value $m(x, 0)$ is zero for all large $x > 0$, then the profile of the solution will tend to the limit steady solution (2.8).
- If $m(x, 0)$ is zero for all large $x > 0$ and there is a small perturbation $h(x_0, t)$ at some large x_0 with $h(x_0, t) \to 0$ as $t \to \infty$, then the solution will track this perturbation and tend to the limit steady solution (2.8) as $t \to \infty$.

Remark 3. For the Camassa–Holm equation

$$m_t + um_x + 2u_x m = 0 \quad \text{with } m = (1 - \partial_x^2)u, \quad \text{in } \mathbb{R},$$

we have $G(x) = \frac{1}{2}e^{-|x|}$ and $G'(0)$ does not exist. However, using tricks similar to those used before, we can obtain the asymptotic stationary equation for the profile of $m(t, x) = \phi(t) f(\phi(t)(x - ct))$:

$$(4f^3 - ff_\eta)f_{\eta\eta\eta} + 2ff_{\eta\eta}^2 - (f_\eta^2 + 22f^2 f_\eta)f_{\eta\eta} + 21ff_\eta^3 = 0 \quad \text{for } \eta \in \mathbb{R}. \tag{4.2}$$

See [18] for details. But this time we are not so lucky as before, as we cannot find the explicit solutions for this equation.

5. Conclusions. We have reported a new phenomenon on the blowup profiles for a modified Camassa–Holm equation (1.1). For (1.1), we have obtained the asymptotic steady equation and its related slow-time self-similar PDEs and found a family of two-parameter steady solutions for the asymptotic steady equation. The standard approach to blowup in both Hamiltonian and parabolic PDEs is to find self-similar solutions in similarity variables based on Lie symmetries of the PDEs, but in this paper, we do not use Lie symmetries. We used the matched asymptotic expansion to get some upstream boundary conditions for the evolution of the solutions in the inner regions. After that, we presented a numerical simulation which shows how the confined initial values evolve toward the Dirac δ momentum: the profile of the solution approaches the family of asymptotic steady solutions very quickly and then it seems to wander through in this family (to the limiting case profile). This is the first time we have seen such a phenomenon in the study of nonlinear PDEs: the PDE has nontrivial dynamics even en route to blowup!

Acknowledgment. We are grateful to the anonymous referees for the comments and suggestions on improving the exposition of this paper and especially for pointing out to us the notion of the self-similarity solution of the second kind.

REFERENCES

[1] M. Alber, R. Camassa, D. D. Holm, and J. E. Marsden, *The geometry of peaked solitons and billiard solutions of a class of integrable PDEs*, Lett. Math. Phys., 32 (1994), pp. 137–151.
[2] M. Alber, R. Camassa, D. D. Holm, and J. E. Marsden, *On the link between umbilic geodesics and soliton solutions of nonlinear PDEs*, Proc. Roy. Soc. London Ser. A, 450 (1995), pp. 677–692.
[3] V. I. Arnold, *Sur la géométrie différentielle des groupes de Lie de dimension infinie et ses applications à l'hydrodynamique des fluides parfaits*, Ann. Inst. Fourier (Grenoble), 16 (1966), pp. 319–361.
[4] V. I. Arnold and B. A. Khesin, *Topological Methods in Hydrodynamics*, Springer-Verlag, New York, 1998.
[5] G. I. Barenblatt, *Scaling, Self-Similarity, and Intermediate Asymptotics*, Cambridge University Press, Cambridge, UK, 1996.
[6] C. J. Budd and J. F. Williams, *Parabolic Monge-Ampère methods for blowup problems in several spatial dimensions*, J. Phys. A, 39 (2006), pp. 5425–5444.
[7] R. Camassa and D. D. Holm, *An integrable shallow water equation with peaked solitons*, Phys. Rev. Lett., 71 (1993), pp. 1661–1664.
[8] R. Camassa, D. D. Holm, and M. Hyman, *A new integrable shallow water equation*, Adv. Appl. Mech., 31 (1994), pp. 1–33.
[9] O. B. Fringer and D. D. Holm, *Integrable vs. nonintegrable geodesic soliton behavior*, Phys. D, 150 (2001), pp. 237–263.
[10] D. D. Holm and J. E. Marsden, *Momentum maps and measure-valued solutions (peakons, filaments, and sheets) for the EPDiff equation*, in The Breadth of Symplectic and Poisson Geometry, Birkhäuser Boston, Boston, 2005, pp. 203–235.
[11] B. Khesin and G. Misiołek, *Euler equations on homogeneous spaces and Virasoro orbits*, Adv. Math., 176 (2003), pp. 116–144.
[12] Y. Martel and F. Merle, *A Liouville theorem for the critical generalized Korteweg-de Vries equation*, J. Math. Pures Appl., 79 (2000), pp. 339–425.
[13] Y. Martel and F. Merle, *Asymptotic stability of solitons of the subcritical gKdV equations revisited*, Nonlinearity, 18 (2005), pp. 723–762.
[14] H. P. McKean, *Fredholm determinants and the Camassa-Holm hierarchy*, Comm. Pure Appl. Math., 56 (2003), pp. 638–680.
[15] R. I. McLachlan and X. Zhang, *Well-posedness of modified Camassa-Holm equations*, J. Differential Equations, 246 (2009), pp. 3241–3259.
[16] M. Van Dyke, *Perturbation Methods in Fluid Mechanics*, The Parabolic Press, Stanford, CA, 1975.
[17] A. I. Volpert, V. A. Volpert, and V. A. Volpert, *Traveling Wave Solutions of Parabolic Systems*, AMS, Providence, RI, 1994.
[18] X. Zhang *Dynamics and numerics of generalised Euler equations*, Ph.D. thesis, Massey University, Palmerston North, New Zealand, 2008.